

Biophysical Journal, Volume 99

Supporting Material

Mechanisms of capsid assembly around a polymer

Aleksandr Kivenson and Michael Hagan

Supporting Information for: Mechanisms of viral capsid assembly around a polymer

Aleksandr Kivenson, Michael F. Hagan

I. MODEL CAPSID GEOMETRIES

The preferred capsid geometries used in this work are cubes with side lengths in the range $N_{\text{side}} \in [7, 12]$, which have respective circumferences of $n_{\text{circ}} \in [24, 44]$. The number of subunits in the lowest energy capsid can be related to the preferred circumference by $N_c = (n_{\text{circ}}/4 + 1)^3 - (n_{\text{circ}}/4 - 1)^3$, which gives $N_c \in [218, 728]$. For the angle tolerance $\delta = \pi/30$ used in this work, it is common for capsids to form as cuboids rather than perfect cubes, with some side lengths longer or shorter by one subunit than the preferred side length; we note that this variability is small compared to the size variability observed for immature retrovirus capsids. As noted in the main text, the interaction geometry ensures that a subunit dimer will have the same interaction free energy for any lattice position and dimer orientation, but in a capsid the 8 corner subunits have one fewer interaction partners than other subunits.

II. POLYMER MODEL DETAILS

Polymer segments occupy only a single lattice site and can have backbone bonds to nearest or next nearest neighbors, with allowed bond lengths of 1 and $\sqrt{2}$, respectively. During dynamics, polymer monomers undergo trial displacements to nearest neighbor lattice sites according to the same algorithm as capsid subunits, with acceptance based on the Metropolis criteria. However, two bonds of length $\sqrt{2}$ may cross, forming an X shape. To preserve non-self-intersecting polymer dynamics, such crossings were explicitly checked for and rejected. All allowed polymer bonds have the same energy in the model.

To maintain computational feasibility with extremely long polymers, some simulations have a box side-length that is shorter than the full extension of the polymer. The side length L was chosen based the relationship between polymer length N_p and the confinement free energy F_{conf} of an unencapsidated polymer $F_{\text{conf}} \cong N_p^{9/4} L^{-15/4}$ [1], to maintain $F_{\text{conf}} \leq 4k_B T$ (which is insignificant compared to total binding energies and entropies) and $L \geq 23$. There were no observed instances of multiple polymer images interacting with an assembling capsid.

Radius of gyration. To verify that this modification of the bond fluctuation model reproduces the statistics of an excluded volume polymer, we measured the average radius of gyration as a function of polymer length. The polymer model exhibits the radius of gyration R_g scaling with length expected for an excluded volume polymer, $R_g \sim N_p^{0.6}$, as shown in Fig. S8. As the strength of attractions increases, the solvent quality decreases from good to theta to poor, as indicated by the

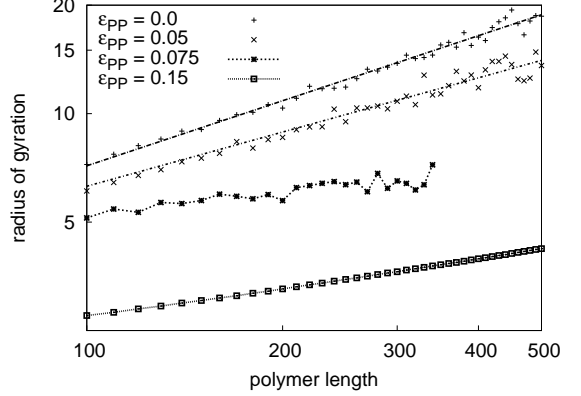


FIG. 8: The average radius of gyration is shown for isolated polymers as a function of N_p for several values of the polymer-polymer attraction ε_{pp} . The solid lines show a fit of the expected scaling for a good solvent: $R_g \sim N_p^{0.6}$ for $\varepsilon_{pp} = 0$ and $R_g \sim N_p^{0.5}$ for $\varepsilon_{pp} = 0.05k_B T$.

scaling of R_g with N_p .

Capsid-polymer interactions. As explained in the main text, a capsid subunit and a polymer segment must satisfy two conditions to experience a favorable interaction. First, the polymer orientation vector, which has length 1 (in units of the lattice spacing) and has its origin at the center of the polymer segment lattice site, must end in the lattice site occupied by capsid subunit. Secondly, the negative of the capsid subunit orientation vector, also of length 1, must end in the lattice site occupied by the polymer segment. This combination restricts interactions between polymer segments and capsid subunits to those that are the 26 nearest, next-nearest, or next-next-nearest neighbors, as is the case for capsid subunit-subunit interactions.

III. SUBUNIT SLIDING ALGORITHM

The one-dimensional diffusion of subunits along the polymer, or subunit sliding, is represented with a special class of Monte Carlo moves in which an adsorbed capsid subunit moves forward or backward by one polymer segment without unbinding from the polymer. As discussed in Refs. [2–6], the one-dimensional diffusion constant is unknown and could vary over a large range depending on the details of how subunits and polymers interact. We therefore consider a range of one-dimensional diffusion constants, which are controlled in our simulations by varying the relative frequencies of subunit sliding moves and ordinary diffusion moves. The probability for choosing a sliding move is given by

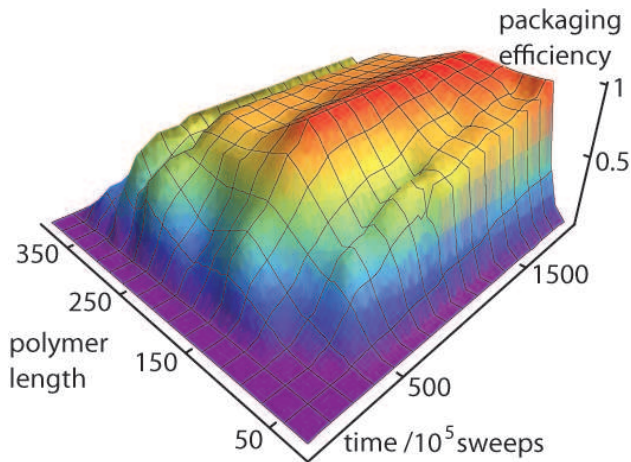


FIG. 9: Packaging efficiencies are shown as a function of time and polymer length N_p for a capsid with a preferred size $N_c = 488$ and $\varepsilon_{pc} = 5.75k_B T$.

$(r_s N_{\text{bound}})/(N_{\text{total}} + r_s N_{\text{bound}})$, where $r_s = D_{1D}/D_{3D}$ is the sliding rate (one-dimensional diffusion constant) relative to the three-dimensional diffusion constant (D_{3D}), N_{bound} is the number of subunits associated with the polymer, and N_{total} is the total number of subunits. Sliding moves do not count toward the number of moves needed for a complete timestep (Monte Carlo sweep).

If a sliding move is selected, a capsid subunit is chosen at random from all the capsid subunits bound to a polymer, and a sliding direction (forward or backward) along the polymer is chosen at random. If no polymer segment exists in that direction, the move is immediately rejected. Otherwise, a new orientation vector is chosen at random from the unit sphere for the polymer segment, the capsid subunit is moved to the lattice site at which the new polymer orientation vector ends, and a new orientation vector for the capsid subunit is chosen from the unit sphere. If the negative of the capsid subunit orientation vector does not end in the lattice site occupied by the polymer segment, the process, starting with choice of orientation vector for the polymer segment, is repeated until the polymer segment and capsid subunit can be bonded according to the criteria listed in the previous section. Finally, a new orientation is chosen from the unit sphere for the polymer subunit that was left behind by the capsomer (this step is necessary to ensure detailed balance). The move is then accepted or rejected based on the total change in energy for all these operations; any subunit-subunit or subunit-segment overlaps that result from the move correspond to infinite energy and lead to rejection.

For polymer bond configurations in which two polymer segments are separated by a single lattice site, it is possible for three-dimensional diffusion moves to move a capsid subunit along the polymer. These moves, which are relatively rare, are not affected by the special sliding moves.

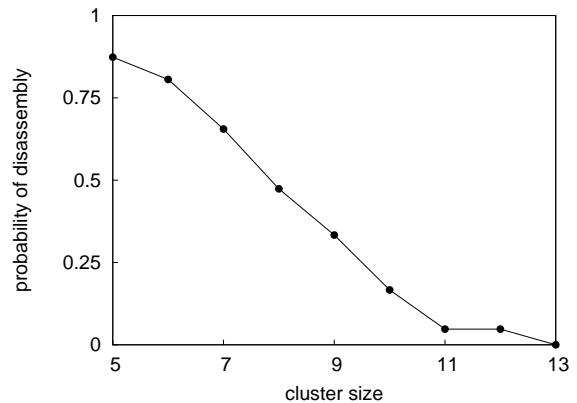


FIG. 10: The probability of partial-capsid intermediate dissolution as a function of cluster size. The fraction of clusters that disassembled (reached size $N \leq 4$) before assembling (reaching size $N \geq 50$) are shown for $N_p = 300$, $\varepsilon_{pc} = 5.75k_B T$, and $N = 488$. Cluster fates were averaged over the assembly trajectories discussed in the main text.

IV. THE TIME DEPENDENCE OF PACKAGING EFFICIENCIES

Packaging efficiencies are shown as functions of time and polymer length in Fig. S9.

V. CAPSID NUCLEATION

We define the critical nucleus size n_{nuc} as the smallest number of assembled subunits that are more likely to assemble than to disassemble. The critical nucleus size was estimated by tracking the fate of clusters in assembly trajectories until they disassemble (defined as reaching a size of $N \leq 4$) or assemble. To expedite the calculation, clusters were defined as assembled upon reaching a size of $N = 50$ subunits, from which subsequent disassembly was never observed for relevant parameters. The disassembly probability is shown as a function of cluster size for representative parameters in Fig. S10, for which the critical nucleus size is 8 subunits. We find that estimated values for the critical nucleus size vary only slightly with polymer length or preferred capsid curvature; since calculated nucleation and growth times are not sensitive to the value of the critical nucleus size, we use $n_{\text{nuc}} = 8$ in all cases.

We note that calculated critical nucleus sizes are only rough estimates for any set of parameters, since the identities of critical nuclei depend on parameters in addition to the number of subunits, such as the number of subunit-subunit bonds, the number of subunit-polymer bonds, and partial capsid configurational entropy – i.e. the intermediate size alone is not sufficient for a good reaction coordinate.

VI. THE DEPENDENCE OF NUCLEATION TIMES ON POLYMER-SUBUNIT INTERACTION STRENGTH

In this section we expand upon the relationships between the polymer-subunit interaction strength ε_{pc} and capsid nucleation times τ_{nuc} given in the main text, and present numbers for some of the parameters. We assume that the system rapidly builds up pre-nucleation intermediates with Boltzmann-weighted concentrations and that nucleation predominantly occurs via the association of individual subunits; both assumptions are good approximations for all conditions in these simulations that yield high packaging efficiencies. With these assumptions, the nucleation rate can be obtained from the concentration of intermediates with the size of one subunit smaller than the critical nucleus size and the rate for one additional subunit to bind. In general, the ensemble of critical nuclei could be defined by number of subunits, number of subunits-subunit bonds, number of subunit-polymer bonds, and the partial capsid configurational entropy (see e.g. Refs. [7, 8]). The analysis is simplified if we neglect partial capsid configurational entropy, and assume that the distribution of partial capsid intermediates with a given number of subunits is sharply peaked around those with the most subunit-subunit bonds and subunit-polymer bonds. Under these assumptions, the concentrations of partial capsid intermediates can be written as a function of only the number of subunits n , and the nucleation rate can be expressed as:

$$\tau_{nuc}^{-1} \simeq k_a c_0 c_{n_{nuc}-1} \quad (3)$$

with c_0 the concentration of free subunits, c_n the concentration of partial capsid intermediates with n subunits adsorbed on the polymer, and k_a the subunit association rate constant.

The concentration of partial capsids adsorbed on the polymer is given by

$$c_n = c_0 N_p \exp[-(G_n + \alpha n g_{pc})/k_B T]. \quad (4)$$

In this expression G_n is the free energy of a capsid intermediate with n subunits, which depends on the number of capsid subunit-subunit bonds, the subunit-subunit interaction strength ε_b , and the subunit binding entropy penalty, which is given by the fraction of subunit orientations available to bound subunits and thus depends on δ . Similarly, $g_{pc} = \varepsilon_{pc} - T s_{pc}$ is the capsid subunit-polymer segment binding free energy with s_{pc} the binding entropy penalty. We calculated $s_{pc}/k_B = -2.56$ by measuring the fraction of subunits bound to polymer segments as a function of c_0 with no subunit-subunit interactions ($\varepsilon_b = 0$). The factor N_p acknowledges that the number of adsorbed intermediates is proportional to the polymer length N_p for a fixed polymer concentration. The parameter α is the number of polymer-subunit interactions per capsid subunit in an adsorbed partial capsid intermediate. By averaging over the ensemble of critical nuclei described in the last section, we obtained $\alpha = 0.81$. Eqs. 3 and 4 imply that capsid nucleation rates should increase exponentially with ε_{pc} . Consistent with this analysis, nucleation rates measured at a range of polymer lengths show a log-linear relationship (see Fig. 6b in the main text) with a slope ≈ 4.6 , independent

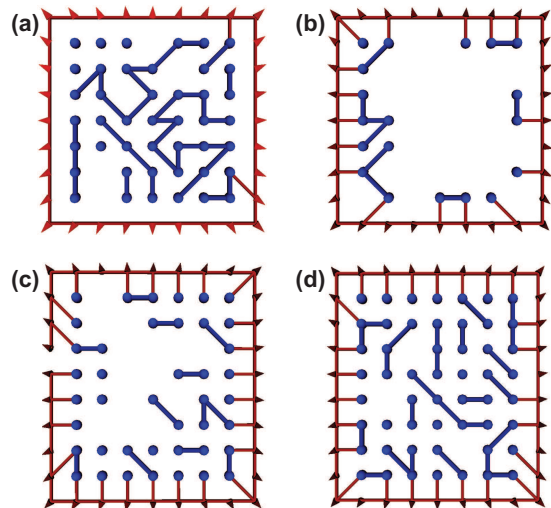


FIG. 11: Conformations of encapsidated polymers. Four views are shown of a polymer encapsidated inside a capsid with a preferred size of 386 subunits. (a) The lattice layer at the inner capsid surface is shown for a configuration with $\varepsilon_{pp} = 0$, $\varepsilon_{pc} = 5.75$, and $N_p = 220$. (b) The lattice layer through the middle of the capsid is shown for the same parameters as (a). (c),(d) The lattice layer through the middle of the capsid is shown for polymer-polymer attractions ($\varepsilon_{pp} = 0.075 k_B T$ and $\varepsilon_{pc} = 5.25 k_B T$) with (c) $N_p = 320$ and (d) $N_p = 410$.

of polymer length. Following Eq. 4 this observation gives $\alpha(n_{nuc} - 1) \approx 4.6$ or a critical nucleus size of $n_{nuc} \approx 6.72$. This number is slightly smaller than the critical nucleus size $n_{nuc} = 8$ obtained from Fig. S10. This discrepancy may result from the assumption that there is one value of n_{nuc} and α for the ensemble of critical nuclei; in fact, larger critical nuclei have smaller values of α .

VII. POLYMER CONFORMATIONS INSIDE THE CAPSID

Conformations of an encapsidated polymer are shown in Fig. S11.

VIII. AN EXTENSION TO THE CAPSID MODEL FOR LOW PREFERRED CURVATURES

The model for capsomer-capsomer binding presented in the main text is sufficient while $\delta < 2\pi/n_{circ}$. For $\delta \geq 2\pi/n_{circ}$, subunit-subunit bonds form if the conditions described in the main text are satisfied OR an alternative set of conditions (see Fig. S12). Although $\delta \geq 2\pi/n_{circ}$ is never considered in this work, we present the alternative set of conditions for completeness:

$$|\theta + 2\pi/n_{circ}| \leq \delta \quad (5)$$

$$\mathbf{r}_j - \mathbf{r}_i = (\arg \max_{\hat{\mathbf{n}}} [\hat{\mathbf{n}} \cdot (-\hat{\mathbf{d}}_b)]) \quad (6)$$

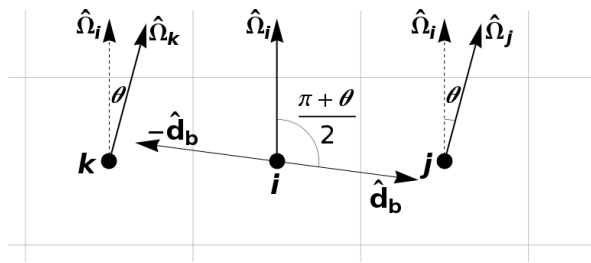


FIG. 12: The geometry of interactions is shown for three model capsid subunits, i , j , and k , where j interacts via the conditions in the main text and k interacts via the alternative conditions. In this illustration, the orientation vectors $\hat{\Omega}_i$, $\hat{\Omega}_j$, and $\hat{\Omega}_k$ are in the plane of the figure and thus the rotation axis $\hat{\Omega}_a$, used to determine \hat{d}_b from $\hat{\Omega}_i$, is perpendicular to that plane. The orientation of the bond vector \hat{d}_b is then determined by the angle θ between the two orientation vectors as described in the main text. (Note that here $\hat{\Omega}_j$ and $\hat{\Omega}_k$ are equal and thus have the same value for θ .) A favorable interaction between i and j will exist if θ satisfies Eq. 1 and a favorable interaction between i and k will exist if θ satisfies Eq. 5.

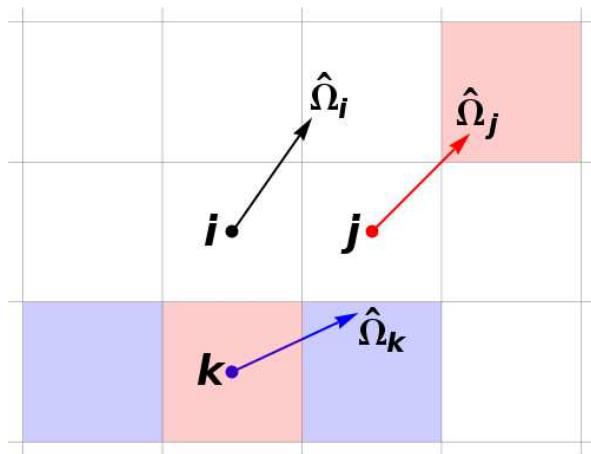


FIG. 13: Definition of capsid subunit exclusion zones. Subunit i could bind to either subunit j or subunit k , but the exclusion zones of subunit j (indicated in red) make it impossible for j and k to be present simultaneously.

IX. CAPSID SUBUNIT EXCLUDED VOLUME

The ‘exclusion zones’ discussed in the main text are illustrated in Fig. S13.

-
- [1] T. Sakaue and E. Raphael, *Macromolecules* **39**, 2621 (2006).
 [2] R. B. Winter, O. G. Berg, and P. H. Vonhippel, *Biochemistry* **20**, 6961 (1981).
 [3] O. G. Berg, R. B. Winter, and P. H. Vonhippel, *Biochemistry* **20**, 6929 (1981).
 [4] T. Hu, A. Y. Grosberg, and B. I. Shklovskii, *Biophysical Journal* **90**, 2731 (2006).
 [5] L. H. Hu, A. Y. Grosberg, and R. Bruinsma, *Biophysical Journal* **95**, 1151 (2008).
 [6] T. Hu and B. I. Shklovskii, *Phys. Rev. E* **75**, 051901 (2007).
 [7] A. C. Pan and D. Chandler, *Journal of Physical Chemistry B* **108**, 19681 (2004).
 [8] D. Moroni, P. R. ten Wolde, and P. G. Bolhuis, *Phys. Rev. Lett.* **94** (2005).